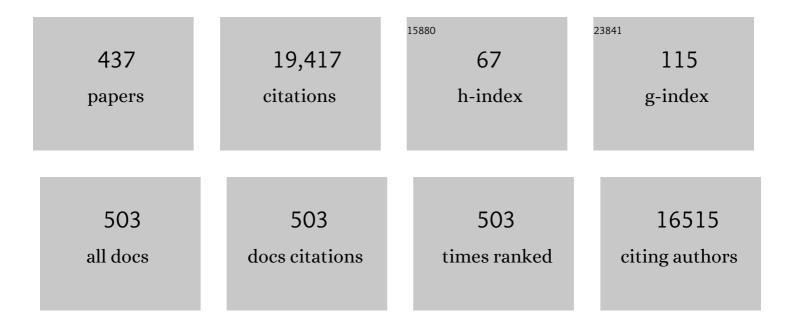
Yukihio Ozaki

List of Publications by Year in descending order

Source: https://exaly.com/author-pdf/4540177/publications.pdf Version: 2024-02-01



Υπκιμίο Οσλεί

#	Article	IF	CITATIONS
1	Surface-enhanced Raman scattering (SERS) Sensing of Biomedicine and Biomolecules. , 2023, , 441-455.		1
2	A new approach to removing interference of moisture from FTIR spectrum. Spectrochimica Acta - Part A: Molecular and Biomolecular Spectroscopy, 2022, 265, 120373.	2.0	11
3	Solvent Effect on Assembling and Interactions in Solutions of Phenol: Infrared Spectroscopic and Density Functional Theory Study. Applied Spectroscopy, 2022, 76, 28-37.	1.2	7
4	Novel Method for Extracting the Spectrum of a Supramolecular Complex via a Comprehensive Approach Involving Two-Dimensional Correlation Spectroscopy, Genetic Algorithm, and Grid Searching. Analytical Chemistry, 2022, 94, 2348-2355.	3.2	3
5	Random swapping, an effective and efficient way to boost the intensities of cross peaks in a 2D asynchronous spectrum. Spectrochimica Acta - Part A: Molecular and Biomolecular Spectroscopy, 2022, 272, 120968.	2.0	0
6	An investigation of the effect of high-pressure on charge transfer in dye-sensitized solar cells based on surface-enhanced Raman spectroscopy. Nanoscale, 2022, 14, 373-381.	2.8	2
7	Experimental verification of increased electronic excitation energy of water in hydrate-melt water by attenuated total reflection-far-ultraviolet spectroscopy. Journal of Chemical Physics, 2022, 156, 074705.	1.2	3
8	Attenuated Total Reflection Far-Ultraviolet (ATR-FUV) Spectroscopy is a Sensitive Tool for Investigation of Protein Adsorption. Applied Spectroscopy, 2022, 76, 793-800.	1.2	1
9	<i>In situ</i> SERS monitoring of intracellular H ₂ O ₂ in single living cells based on label-free bifunctional Fe ₃ O ₄ @Ag nanoparticles. Analyst, The, 2022, 147, 1815-1823.	1.7	9
10	Progress of tip-enhanced Raman scattering for the last two decades and its challenges in very recent years. Nanoscale, 2022, 14, 5265-5288.	2.8	18
11	NIR spectroscopy – What a wonderful world!. NIR News, 2022, 33, 10-17.	1.6	1
12	A Study of C=O…HO and OH…OH (Dimer, Trimer, and Oligomer) Hydrogen Bonding in a Poly(4-vinylphenol) 30%/Poly(methyl methacrylate) 70% Blend and its Thermal Behavior Using Near-Infrared Spectroscopy and Infrared Spectroscopy. Applied Spectroscopy, 2022, 76, 831-840.	1.2	2
13	3D SERS Imaging of Nanoporous Gold–Silver Microstructures: Exploring the Formation Mechanism Based on Galvanic Replacement Reaction. Journal of Physical Chemistry C, 2022, 126, 5617-5627.	1.5	2
14	Two types of C Oâ‹~HO hydrogen bonds and OHâ‹~OH (dimer, trimer, oligomer) hydrogen bonds in PVA with 88% saponification/PMMA and PVA with 99% saponification/PMMA blends and their thermal behavior studied by infrared spectroscopy. Polymer, 2022, 246, 124725.	1.8	14
15	Association and solubility of chlorophenols in CCl4: MIR/NIR spectroscopic and DFT study. Spectrochimica Acta - Part A: Molecular and Biomolecular Spectroscopy, 2022, 274, 121077.	2.0	0
16	Determination of the Influence of Various Factors on the Character of Surface Functionalization of Copper(I) and Copper(II) Oxide Nanosensors with Phenylboronic Acid Derivatives. Langmuir, 2022, 38, 557-568.	1.6	2
17	New Insights of Charge Transfer at Metal/Semiconductor Interfaces for Hot-Electron Generation Studied by Surface-Enhanced Raman Spectroscopy. Journal of Physical Chemistry Letters, 2022, 13, 3571-3578.	2.1	4
18	Deprotonation from an OH on <i>myo</i> -Inositol Promoted by μ ₂ -Bridges with Possible Regioselectivity/Chiral Selectivity. Inorganic Chemistry, 2022, 61, 6138-6148.	1.9	1

#	Article	IF	CITATIONS
19	Development of an amino acid sequence-dependent analytical method for peptides using near-infrared spectroscopy. Analyst, The, 2022, 147, 3634-3642.	1.7	6
20	In-situ fingerprinting phosphorylated proteins via surface-enhanced Raman spectroscopy: Single-site discrimination of Tau biomarkers in Alzheimer's disease. Biosensors and Bioelectronics, 2021, 171, 112748.	5.3	22
21	Method of Monitoring the Number of Amide Bonds in Peptides Using Near-Infrared Spectroscopy. Analytical Chemistry, 2021, 93, 2758-2766.	3.2	9
22	Intensity Enhancement of a Two-Dimensional Asynchronous Spectrum Without Noise Level Fluctuation Escalation Using a One-Dimensional Spectra Sequence Change. Applied Spectroscopy, 2021, 75, 422-433.	1.2	7
23	Recent advances in surfaceâ€enhanced Raman scatteringâ€based sensors for the detection of inorganic ions: Sensing mechanism and beyond. Journal of Raman Spectroscopy, 2021, 52, 468-481.	1.2	22
24	Advances, challenges and perspectives of quantum chemical approaches in molecular spectroscopy of the condensed phase. Chemical Society Reviews, 2021, 50, 10917-10954.	18.7	34
25	Solvent effect on the competition between weak and strong interactions in phenol solutions studied by near-infrared spectroscopy and DFT calculations. Physical Chemistry Chemical Physics, 2021, 23, 19188-19194.	1.3	9
26	Half-raspberry-like bimetallic nanoassembly: Interstitial dependent correlated surface plasmon resonances and surface-enhanced Raman spectroscopy. Physical Chemistry Chemical Physics, 2021, 23, 23875-23885.	1.3	4
27	Investigation on the luminescence behavior of terbium acetylsalicylate/bilirubin system via 2D-COS approaches. Spectrochimica Acta - Part A: Molecular and Biomolecular Spectroscopy, 2021, 251, 119427.	2.0	6
28	ATR-far-ultraviolet spectroscopy in the condensed phase—The present status and future perspectives. Spectrochimica Acta - Part A: Molecular and Biomolecular Spectroscopy, 2021, 253, 119549.	2.0	14
29	Electric field analysis, polarization, excitation wavelength dependence, and novel applications of tipâ€enhanced Raman scattering. Journal of Raman Spectroscopy, 2021, 52, 1997-2017.	1.2	7
30	Understanding phase transition and vibrational mode coupling in ammonium nitrate using 2D correlation Raman spectroscopy. Spectrochimica Acta - Part A: Molecular and Biomolecular Spectroscopy, 2021, 254, 119581.	2.0	9
31	Anharmonic DFT Study of Near-Infrared Spectra of Caffeine: Vibrational Analysis of the Second Overtones and Ternary Combinations. Molecules, 2021, 26, 5212.	1.7	12
32	Infrared Spectroscopy—Mid-infrared, Near-infrared, and Far-infrared/Terahertz Spectroscopy. Analytical Sciences, 2021, 37, 1193-1212.	0.8	42
33	Far-Ultraviolet Spectroscopy and Quantum Chemical Calculation Studies of the Conformational Dependence on the Electronic Structure and Transitions of Cyclohexane, Methyl and Dimethyl Cyclohexane, and Decalin; Effects of Axial Substitutions on the Electronic Transitions. Journal of Physical Chemistry A. 2021, 125, 8205-8214.	1.1	3
34	Effect of Raman exposure time on the quantitative and discriminant analyses of carotenoid concentrations in intact tomatoes. Food Chemistry, 2021, 360, 129896.	4.2	12
35	MCR-ALS with sample insertion constraint to enhance the sensitivity of surface-enhanced Raman scattering detection. Analyst, The, 2021, 146, 3251-3262.	1.7	8
36	Hollow Multi‣helled V ₂ O ₅ Microstructures Integrating Multiple Synergistic Resonances for Enhanced Semiconductor SERS. Advanced Optical Materials, 2021, 9, 2101866.	3.6	22

#	Article	IF	CITATIONS
37	Editorial: Novel SERS-Active Materials and Substrates: Sensing and (Bio)applications. Frontiers in Chemistry, 2021, 9, 784735.	1.8	0
38	Surface-enhanced Raman spectroscopy. Nature Reviews Methods Primers, 2021, 1, .	11.8	183
39	Present and Future of Surface-Enhanced Raman Scattering. ACS Nano, 2020, 14, 28-117.	7.3	2,153
40	Sample–Sample Correlation Asynchronous Spectroscopic Method Coupled with Multivariate Curve Resolution-Alternating Least Squares To Analyze Challenging Bilinear Data. Analytical Chemistry, 2020, 92, 1477-1484.	3.2	12
41	lodine staining as a useful probe for distinguishing insulin amyloid polymorphs. Scientific Reports, 2020, 10, 16741.	1.6	8
42	Nitrosonaphthol reaction-assisted SERS assay for selective determination of 5-hydroxyindole-3-acetic acid in human urine. Analytica Chimica Acta, 2020, 1134, 34-40.	2.6	10
43	Exploration of Insulin Amyloid Polymorphism Using Raman Spectroscopy and Imaging. Biophysical Journal, 2020, 118, 2997-3007.	0.2	12
44	Accurate Monitoring Platform for the Surface Catalysis of Nanozyme Validated by Surface-Enhanced Raman-Kinetics Model. Analytical Chemistry, 2020, 92, 11763-11770.	3.2	36
45	Identification of systematic absence of cross-peaks (SACPs) in a two-dimensional asynchronous Spectrum using an auxiliary 2D quotient Spectrum and a statistical test. Spectrochimica Acta - Part A: Molecular and Biomolecular Spectroscopy, 2020, 243, 118789.	2.0	11
46	A Chiralâ€Labelâ€Free SERS Strategy for the Synchronous Chiral Discrimination and Identification of Small Aromatic Molecules. Angewandte Chemie - International Edition, 2020, 59, 19079-19086.	7.2	40
47	A Chiralâ€Labelâ€Free SERS Strategy for the Synchronous Chiral Discrimination and Identification of Small Aromatic Molecules. Angewandte Chemie, 2020, 132, 19241-19248.	1.6	7
48	SERS Blinking on Anisotropic Nanoparticles. Journal of Physical Chemistry C, 2020, 124, 20328-20339.	1.5	5
49	Innentitelbild: A Chiral‣abelâ€Free SERS Strategy for the Synchronous Chiral Discrimination and Identification of Small Aromatic Molecules (Angew. Chem. 43/2020). Angewandte Chemie, 2020, 132, 18982-18982.	1.6	0
50	Attenuated total reflectance far-ultraviolet and deep-ultraviolet spectroscopy analysis of the electronic structure of a dicyanamide-based ionic liquid with Li ⁺ . Physical Chemistry Chemical Physics, 2020, 22, 21768-21775.	1.3	7
51	Theoretical Modeling of Electronic Structures of Polyiodide Species Included in α-Cyclodextrin. Journal of Physical Chemistry B, 2020, 124, 4089-4096.	1.2	13
52	Assessment of Embryonic Bioactivity through Changes in the Water Structure Using Near-Infrared Spectroscopy and Imaging. Analytical Chemistry, 2020, 92, 8133-8141.	3.2	14
53	Distinguishing Enantiomers by Tipâ€Enhanced Raman Scattering: Chemically Modified Silver Tip with an Asymmetric Atomic Arrangement. Angewandte Chemie - International Edition, 2020, 59, 14564-14569.	7.2	9
54	Enhanced Surface Plasmon Resonance Wavelength Shifts by Molecular Electronic Absorption in Far- and Deep-Ultraviolet Regions. Scientific Reports, 2020, 10, 9938.	1.6	14

#	Article	IF	CITATIONS
55	Distinguishing Enantiomers by Tipâ€Enhanced Raman Scattering: Chemically Modified Silver Tip with an Asymmetric Atomic Arrangement. Angewandte Chemie, 2020, 132, 14672-14677.	1.6	1
56	Lipid Droplet Composition Varies Based on Medaka Fish Eggs Development as Revealed by NIR-, MIR-, and Raman Imaging. Molecules, 2020, 25, 817.	1.7	12
57	Near-infrared spectroscopy and imaging in protein research. , 2020, , 143-176.		10
58	Interactions Between Epitaxial Graphene Grown on the Si- and C-Faces of 4H-SiC Investigated Using Raman Imaging and Tip-Enhanced Raman Scattering. Applied Spectroscopy, 2020, 74, 1384-1390.	1.2	4
59	Glucose Monitoring in Cell Culture with Online Ultrasound-Assisted Near-Infrared Spectroscopy. Analytical Chemistry, 2020, 92, 2946-2952.	3.2	15
60	Solvation effects on wavenumbers and absorption intensities of the OH-stretch vibration in phenolic compounds – electrical- and mechanical anharmonicity <i>via</i> a combined DFT/Numerov approach. Physical Chemistry Chemical Physics, 2020, 22, 13017-13029.	1.3	14
61	Advances in Molecular Spectroscopy in Condensed Phase and Quantum Chemistry. Molecular Science, 2020, 14, A0114.	0.2	0
62	Reusable Silicon-Based SERS Chip for Ratiometric Analysis of Fluoride Ion in Aqueous Solutions. ACS Sensors, 2019, 4, 2336-2342.	4.0	34
63	Plasmon-Enhanced Optical Tweezers for Single Molecules on and near a Colloidal Silver Nanoaggregate. Journal of Physical Chemistry C, 2019, 123, 18001-18006.	1.5	21
64	Enhanced Raman Scattering by ZnO Superstructures: Synergistic Effect of Charge Transfer and Mie Resonances. Angewandte Chemie - International Edition, 2019, 58, 14452-14456.	7.2	133
65	A chiral signal-amplified sensor for enantioselective discrimination of amino acids based on charge transfer-induced SERS. Chemical Communications, 2019, 55, 9697-9700.	2.2	29
66	Enhanced Raman Scattering by ZnO Superstructures: Synergistic Effect of Charge Transfer and Mie Resonances. Angewandte Chemie, 2019, 131, 14594-14598.	1.6	15
67	Innenrücktitelbild: Enhanced Raman Scattering by ZnO Superstructures: Synergistic Effect of Charge Transfer and Mie Resonances (Angew. Chem. 41/2019). Angewandte Chemie, 2019, 131, 14915-14915.	1.6	0
68	Crystallization of poly(3â€hydroxybutyrate― <i>co</i> â€3â€hydroxyhexanoate) during melt extrusion promoted by residual crystals. Polymer Crystallization, 2019, 2, e10076.	0.5	6
69	Functional nanomaterials with unique enzyme-like characteristics for sensing applications. Journal of Materials Chemistry B, 2019, 7, 850-875.	2.9	155
70	IR Spectra of Crystalline Nucleobases: Combination of Periodic Harmonic Calculations with Anharmonic Corrections Based on Finite Models. Journal of Physical Chemistry B, 2019, 123, 10001-10013.	1.2	18
71	Phosphoric acid and phosphorylation levels are potential biomarkers indicating developmental competence of matured oocytes. Analyst, The, 2019, 144, 1527-1534.	1.7	7
72	CTAB-triggered Ag aggregates for reproducible SERS analysis of urinary polycyclic aromatic hydrocarbon metabolites. Chemical Communications, 2019, 55, 2146-2149.	2.2	30

#	Article	IF	CITATIONS
73	A novel systematic absence of cross peaks-based 2D-COS approach for bilinear data. Spectrochimica Acta - Part A: Molecular and Biomolecular Spectroscopy, 2019, 220, 117103.	2.0	19
74	Low-Frequency Vibrational Modes of Nylon 6 Studied by Using Infrared and Raman Spectroscopies and Density Functional Theory Calculations. Journal of Physical Chemistry B, 2019, 123, 5368-5376.	1.2	23
75	Recent Advances in Molecular Spectroscopy of Electronic and Vibrational Transitions in Condensed Phase and Its Application to Chemistry. Bulletin of the Chemical Society of Japan, 2019, 92, 629-654.	2.0	28
76	A Novel Approach Based on Two-Dimensional Correlation Spectroscopy to Determine the Stoichiometric Ratio of Two Substances Involved in Intermolecular Interactions. Applied Spectroscopy, 2019, 73, 1051-1060.	1.2	12
77	Overtones of νC≡N Vibration as a Probe of Structure of Liquid CH ₃ CN, CD ₃ CN, and CCl ₃ CN: Combined Infrared, Near-Infrared, and Raman Spectroscopic Studies with Anharmonic Density Functional Theory Calculations. Journal of Physical Chemistry A, 2019, 123, 4431-4442.	1.1	27
78	A preliminary study on constructing a high-dimensional asynchronous spectrum to analyze bilinear data. Spectrochimica Acta - Part A: Molecular and Biomolecular Spectroscopy, 2019, 216, 76-84.	2.0	14
79	Effect of TiO 2 on Altering Direction of Interfacial Charge Transfer in a TiO 2 â€Agâ€MPYâ€FePc System by SERS. Angewandte Chemie, 2019, 131, 8256-8260.	1.6	12
80	Effect of TiO ₂ on Altering Direction of Interfacial Charge Transfer in a TiO ₂ â€Agâ€MPYâ€FePc System by SERS. Angewandte Chemie - International Edition, 2019, 58, 8172-8176.	7.2	66
81	Distinct Difference in Sensitivity of NIR vs. IR Bands of Melamine to Inter-Molecular Interactions with Impact on Analytical Spectroscopy Explained by Anharmonic Quantum Mechanical Study. Molecules, 2019, 24, 1402.	1.7	38
82	Simulated NIR spectra as sensitive markers of the structure and interactions in nucleobases. Scientific Reports, 2019, 9, 17398.	1.6	20
83	NIR spectroscopy research in the Ozaki group for the last 30 years. NIR News, 2019, 30, 16-20.	1.6	1
84	Nickel Nanowires Combined with Surface-Enhanced Raman Spectroscopy: Application in Label-Free Detection of Cytochrome c-Mediated Apoptosis. Analytical Chemistry, 2019, 91, 1213-1216.	3.2	24
85	FT-IR Spectroscopic Imaging of Endothelial Cells Response to Tumor Necrosis Factor-α: To Follow Markers of Inflammation Using Standard and High-Magnification Resolution. Analytical Chemistry, 2018, 90, 3727-3736.	3.2	12
86	<i>In situ</i> formation of SERS hot spots by a bis-quaternized perylene dye: a simple strategy for highly sensitive detection of heparin over a wide concentration range. Analyst, The, 2018, 143, 1899-1905.	1.7	21
87	Noninvasive, highâ€speed, nearâ€infrared imaging of the biomolecular distribution and molecular mechanism of embryonic development in fertilized fish eggs. Journal of Biophotonics, 2018, 11, e201700115.	1.1	17
88	Three different kinds of weak C-Hâ⊄O=C inter- and intramolecular interactions in poly(ε-caprolactone) studied by using terahertz spectroscopy, infrared spectroscopy and quantum chemical calculations. Polymer, 2018, 137, 245-254.	1.8	44
89	Tip-Enhanced Raman Scattering in Liquid/Solution. , 2018, , 299-321.		3
90	Exploring the difference in xerogels and organogels through <i>in situ</i> observation. Royal Society Open Science, 2018, 5, 170492.	1.1	6

#	Article	IF	CITATIONS
91	An Application for the Quantitative Analysis of Pharmaceutical Tablets Using a Rapid Switching System Between a Near-Infrared Spectrometer and a Portable Near-Infrared Imaging System Equipped with Fiber Optics. Applied Spectroscopy, 2018, 72, 551-561.	1.2	14
92	Novel Method of Constructing Two-Dimensional Correlation Spectroscopy without Subtracting a Reference Spectrum. Journal of Physical Chemistry A, 2018, 122, 788-797.	1.1	19
93	Nonstaining Blood Flow Imaging Using Optical Interference Due to Doppler Shift and Near-Infrared Imaging of Molecular Distribution in Developing Fish Egg Embryos. Analytical Chemistry, 2018, 90, 5217-5223.	3.2	19
94	Excitation wavelength selection for quantitative analysis of carotenoids in tomatoes using Raman spectroscopy. Food Chemistry, 2018, 258, 308-313.	4.2	37
95	Rydberg transitions as a probe for structural changes and phase transition at polymer surfaces: an ATR-FUV-DUV and quantum chemical study of poly(3-hydroxybutyrate) and its nanocomposite with graphene. Physical Chemistry Chemical Physics, 2018, 20, 8859-8873.	1.3	20
96	Advances in Far-Ultraviolet Spectroscopy in the Solid and Liquid States. , 2018, , 251-285.		12
97	Study on phase separation in an ultra-thin poly(methyl methacrylate)/poly(4-vinyl phenol) film by infrared reflection absorption spectroscopy. Polymer, 2018, 135, 69-75.	1.8	4
98	Electronic Spectra of Graphene in Far- and Deep-Ultraviolet Region: Attenuated Total Reflection Spectroscopy and Quantum Chemical Calculation Study. Journal of Physical Chemistry C, 2018, 122, 28998-29008.	1.5	9
99	Blinking Surface-Enhanced Raman Scattering and Fluorescence From a Single Silver Nanoaggregate Simultaneously Analyzed by Bi-Color Intensity Ratios and a Truncated Power Law. Journal of Physical Chemistry C, 2018, 122, 22106-22113.	1.5	7
100	Design of a Novel Apparatus to Enrich Analytes via a Diffuse-Evaporation Process for HPLC-FTIR Analysis. Analytical Sciences, 2018, 34, 1351-1356.	0.8	3
101	Investigation of charge-transfer between a 4-mercaptobenzoic acid monolayer and TiO ₂ nanoparticles under high pressure using surface-enhanced Raman scattering. Chemical Communications, 2018, 54, 6280-6283.	2.2	27
102	A dual colorimetric and SERS detection of Hg2+ based on the stimulus of intrinsic oxidase-like catalytic activity of Ag-CoFe2O4/reduced graphene oxide nanocomposites. Chemical Engineering Journal, 2018, 350, 120-130.	6.6	87
103	Local structural changes in graphene oxide layers induced by silver nanoparticles. Physical Chemistry Chemical Physics, 2018, 20, 21498-21505.	1.3	4
104	Reduced Charge-Transfer Threshold in Dye-Sensitized Solar Cells with an Au@Ag/N3/ <i>n</i> -TiO ₂ Structure As Revealed by Surface-Enhanced Raman Scattering. Journal of Physical Chemistry C, 2018, 122, 12748-12760.	1.5	13
105	NIR Spectra Simulations by Anharmonic DFT-Saturated and Unsaturated Long-Chain Fatty Acids. Journal of Physical Chemistry B, 2018, 122, 6931-6944.	1.2	39
106	Recent Developments in Plasmon-Supported Raman Spectroscopy. , 2018, , .		22
107	Unsaturated lipid bodies as a hallmark of inflammation studied by Raman 2D and 3D microscopy. Scientific Reports, 2017, 7, 40889.	1.6	75
108	Low-Frequency Vibrational Modes of Poly(glycolic acid) and Thermal Expansion of Crystal Lattice Assigned On the Basis of DFT-Spectral Simulation Aided with a Fragment Method. Journal of Physical Chemistry B, 2017, 121, 1128-1138.	1.2	33

#	Article	IF	CITATIONS
109	Analysis of blinking from multicoloured SERSâ€active Ag colloidal nanoaggregates with polyâ€Lâ€lysine via truncated power law. Journal of Raman Spectroscopy, 2017, 48, 570-577.	1.2	9
110	Semiconductor-enhanced Raman scattering: active nanomaterials and applications. Nanoscale, 2017, 9, 4847-4861.	2.8	289
111	Terahertz Imaging of the Distribution of Crystallinity and Crystalline Orientation in a Poly(É>-caprolactone) Film. Applied Spectroscopy, 2017, 71, 1537-1542.	1.2	17
112	Charge Transfer at the TiO ₂ /N3/Ag Interface Monitored by Surface-Enhanced Raman Spectroscopy. Journal of Physical Chemistry C, 2017, 121, 5145-5153.	1.5	11
113	Influence of Non-fundamental Modes on Mid-infrared Spectra: Anharmonic DFT Study of Aliphatic Ethers. Journal of Physical Chemistry A, 2017, 121, 1412-1424.	1.1	27
114	Facile synthesis of silver nanoparticles/carbon dots for a charge transfer study and peroxidase-like catalytic monitoring by surface-enhanced Raman scattering. Applied Surface Science, 2017, 410, 42-50.	3.1	34
115	Non-destructive monitoring of mouse embryo development and its qualitative evaluation at the molecular level using Raman spectroscopy. Scientific Reports, 2017, 7, 43942.	1.6	25
116	Changes in the Electronic States of Low-Temperature Solid <i>n</i> -Tetradecane: Decrease in the HOMO–LUMO Gap. ACS Omega, 2017, 2, 618-625.	1.6	25
117	Distribution of Polymorphic Crystals in the Ring-Banded Spherulites of Poly(butylene adipate) Studied Using High-Resolution Raman Imaging. Macromolecules, 2017, 50, 3377-3387.	2.2	18
118	The Born-Oppenheimer molecular simulations of infrared spectra of crystalline poly-(R)-3-hydroxybutyrate with analysis of weak C H⋯O C hydrogen bonds. Chemical Physics Letters, 2017, 678, 112-118.	1.2	11
119	Correlations between Structure and Near-Infrared Spectra of Saturated and Unsaturated Carboxylic Acids. Insight from Anharmonic Density Functional Theory Calculations. Journal of Physical Chemistry A, 2017, 121, 3437-3451.	1.1	64
120	Reinvestigation of the β-to-α Crystal Phase Transition of Poly(butylene adipate) by the Time-Resolved X-ray Scattering and FTIR Spectral Measurements in the Temperature-Jump Process. Macromolecules, 2017, 50, 3883-3889.	2.2	35
121	Polarization dependence of tip-enhanced Raman and plasmon-resonance Rayleigh scattering spectra. Applied Physics Letters, 2017, 110, 233104.	1.5	7
122	Spectra-structure correlations of saturated and unsaturated medium-chain fatty acids. Near-infrared and anharmonic DFT study of hexanoic acid and sorbic acid. Spectrochimica Acta - Part A: Molecular and Biomolecular Spectroscopy, 2017, 185, 35-44.	2.0	38
123	Investigation on intermolecular interaction between berberine and β-cyclodextrin by 2D UV–Vis asynchronous spectra. Spectrochimica Acta - Part A: Molecular and Biomolecular Spectroscopy, 2017, 185, 343-348.	2.0	18
124	Critical Evaluation of NIR and ATR-IR Spectroscopic Quantifications of Rosmarinic Acid in Rosmarini folium Supported by Quantum Chemical Calculations. Planta Medica, 2017, 83, 1076-1084.	0.7	25
125	Temperature Drift of Conformational Equilibria of Butyl Alcohols Studied by Near-Infrared Spectroscopy and Fully Anharmonic DFT. Journal of Physical Chemistry A, 2017, 121, 1950-1961.	1.1	48
126	Infrared Spectroscopy and Born–Oppenheimer Molecular Dynamics Simulation Study on Deuterium Substitution in the Crystalline Benzoic Acid. Journal of Physical Chemistry B, 2017, 121, 479-489.	1.2	9

#	Article	IF	CITATIONS
127	Critical evaluation of spectral information of benchtop vs. portable near-infrared spectrometers: quantum chemistry and two-dimensional correlation spectroscopy for a better understanding of PLS regression models of the rosmarinic acid content in Rosmarini folium. Analyst, The, 2017, 142, 455-464.	1.7	94
128	Rapid analysis of chemical composition in intact and milled rice cookies using near infrared spectroscopy. Journal of Near Infrared Spectroscopy, 2017, 25, 330-337.	0.8	17
129	Spectroscopic and Quantum Mechanical Calculation Study of the Effect of Isotopic Substitution on NIR Spectra of Methanol. Journal of Physical Chemistry A, 2017, 121, 7925-7936.	1.1	29
130	Investigation on the Behavior of Noise in Asynchronous Spectra in Generalized Two-Dimensional (2D) Correlation Spectroscopy and Application of Butterworth Filter in the Improvement of Signal-to-Noise Ratio of 2D Asynchronous Spectra. Journal of Physical Chemistry A, 2017, 121, 7524-7533.	1.1	21
131	Unveiling the Aggregation of Lycopene in Vitro and in Vivo: UV–Vis, Resonance Raman, and Raman Imaging Studies. Journal of Physical Chemistry B, 2017, 121, 8046-8057.	1.2	35
132	Interpretation of the à ↕X̃ transition of hydrated protons in aqueous solutions observed in the far-UV region with quantum chemical calculations. Physical Chemistry Chemical Physics, 2017, 19, 21490-21499.	1.3	6
133	Temperature compensation for determination of moisture and reducing sugar of longan honey by near infrared spectroscopy. Journal of Near Infrared Spectroscopy, 2017, 25, 36-44.	0.8	18
134	Measurement of pH-dependent surface-enhanced hyper-Raman scattering at desired positions on yeast cells via optical trapping. Analyst, The, 2017, 142, 3967-3974.	1.7	10
135	An enhanced degree of charge transfer in dye-sensitized solar cells with a ZnO-TiO ₂ /N3/Ag structure as revealed by surface-enhanced Raman scattering. Nanoscale, 2017, 9, 15303-15313.	2.8	36
136	Far- and deep-ultraviolet surface plasmon resonance sensors working in aqueous solutions using aluminum thin films. Scientific Reports, 2017, 7, 5934.	1.6	38
137	Non-staining visualization of embryogenesis and energy metabolism in medaka fish eggs using near-infrared spectroscopy and imaging. Analyst, The, 2017, 142, 4765-4772.	1.7	14
138	Biological application of water-based electrochemically synthesized CuO leaf-like arrays: SERS response modulated by the positional isomerism and interface type. Physical Chemistry Chemical Physics, 2017, 19, 31842-31855.	1.3	7
139	Plasmon-enhanced spectroscopy of absorption and spontaneous emissions explained using cavity quantum optics. Chemical Society Reviews, 2017, 46, 3904-3921.	18.7	113
140	Characterization of Thermal Oxides on 4H-SiC Epitaxial Substrates Using Fourier-Transform Infrared Spectroscopy, 2017, 71, 911-918.	1.2	6
141	High-Speed Scanning for the Quantitative Evaluation of Glycogen Concentration in Bioethanol Feedstock <i>Synechocystis</i> sp. PCC6803 Using a Near-Infrared Hyperspectral Imaging System with a New Near-Infrared Spectral Camera. Applied Spectroscopy, 2017, 71, 463-471.	1.2	5
142	Quantum chemical calculation of NIR spectra of practical materials. NIR News, 2017, 28, 13-20.	1.6	12
143	Rapid and nondestructive analysis of deep-fried taro chip qualities using near infrared spectroscopy. Journal of Near Infrared Spectroscopy, 2017, 25, 127-137.	0.8	6
144	New Application of Far-ultraviolet Spectroscopy. Bunseki Kagaku, 2017, 66, 319-331.	0.1	0

#	Article	IF	CITATIONS
145	Crystallization of ultrathin poly(3-hydroxybutyrate) films in blends with small amounts of poly(<scp>l</scp> -lactic acid): correlation between film thickness and molecular weight of poly(<scp>l</scp> -lactic acid). RSC Advances, 2017, 7, 52651-52660.	1.7	2
146	In Vivo Monitoring of the Growth of Fertilized Eggs of Medaka Fish (Oryzias latipes) by Near-Infrared Spectroscopy and Near-Infrared Imaging—A Marked Change in the Relative Content of Weakly Hydrogen-Bonded Water in Egg Yolk Just before Hatching. Molecules, 2016, 21, 1003.	1.7	23
147	Introduction of Quantum Chemical Calculation for near Infrared Spectroscopy. NIR News, 2016, 27, 8-11.	1.6	1
148	Direct optical measurements of far- and deep-ultraviolet surface plasmon resonance with different refractive indices. Optics Express, 2016, 24, 21886.	1.7	28
149	3D SERS Imaging Using Chemically Synthesized Highly Symmetric Nanoporous Silver Microparticles. Angewandte Chemie - International Edition, 2016, 55, 8391-8395.	7.2	44
150	Surface-enhanced resonance Raman scattering of hemoproteins and those in complicated biological systems. Analyst, The, 2016, 141, 5020-5036.	1.7	28
151	Side-illuminated tip-enhanced Raman study of edge phonon in graphene at the electrical breakdown limit. Applied Physics Letters, 2016, 108, .	1.5	7
152	Charge-Transfer-Induced Enantiomer Selective Discrimination of Chiral Alcohols by SERS. Journal of Physical Chemistry C, 2016, 120, 29374-29381.	1.5	28
153	Near-Infrared Spectroscopy and Imaging Studies of Fertilized Fish Eggs: In Vivo Monitoring of Egg Growth at the Molecular Level. Scientific Reports, 2016, 6, 20066.	1.6	38
154	Darkfield microspectroscopy of nanostructures on silver tip-enhanced Raman scattering probes. Applied Physics Letters, 2016, 108, .	1.5	15
155	Synthesis of bifunctional reduced graphene oxide/CuS/Au composite nanosheets for in situ monitoring of a peroxidase-like catalytic reaction by surface-enhanced Raman spectroscopy. RSC Advances, 2016, 6, 54456-54462.	1.7	45
156	C–Hâ√O (ether) hydrogen bonding along the (110) direction in polyglycolic acid studied by infrared spectroscopy, wide-angle X-ray diffraction, quantum chemical calculations and natural bond orbital calculations. RSC Advances, 2016, 6, 16817-16823.	1.7	37
157	Born–Oppenheimer Molecular Dynamics Study on Proton Dynamics of Strong Hydrogen Bonds in Aspirin Crystals, with Emphasis on Differences between Two Crystal Forms. Journal of Physical Chemistry B, 2016, 120, 3854-3862.	1.2	24
158	A spectroscopic and theoretical study in the near-infrared region of low concentration aliphatic alcohols. Physical Chemistry Chemical Physics, 2016, 18, 13666-13682.	1.3	72
159	Higher-order structure formation of a poly(3-hydroxybutyrate) film during solvent evaporation. RSC Advances, 2016, 6, 95021-95031.	1.7	3
160	Spectroscopic and Computational Study of Acetic Acid and Its Cyclic Dimer in the Near-Infrared Region. Journal of Physical Chemistry A, 2016, 120, 6170-6183.	1.1	44
161	Semiconductor materials in analytical applications of surfaceâ€enhanced Raman scattering. Journal of Raman Spectroscopy, 2016, 47, 51-58.	1.2	127
162	Computational and quantum chemical study on high-frequency dielectric function of tert-butylmethyl ether in mid-infrared and near-infrared regions. Journal of Molecular Liquids, 2016, 224, 1189-1198.	2.3	9

#	Article	IF	CITATIONS
163	Electronic absorption spectra of imidazolium-based ionic liquids studied by far-ultraviolet spectroscopy and quantum chemical calculations. Physical Chemistry Chemical Physics, 2016, 18, 22526-22530.	1.3	48
164	Far- and deep-ultraviolet spectroscopic investigations for titanium dioxide: electronic absorption, Rayleigh scattering, and Raman spectroscopy. Journal of Materials Chemistry C, 2016, 4, 7706-7717.	2.7	36
165	<i>In Vivo</i> Monitoring of Fertilised Fish Egg Growth by near Infrared Spectroscopy and Imaging. NIR News, 2016, 27, 7-10.	1.6	6
166	Evolution of Intermediate and Highly Ordered Crystalline States under Spatial Confinement in Poly(3-hydroxybutyrate) Ultrathin Films. Macromolecules, 2016, 49, 4202-4210.	2.2	23
167	Ultrasensitive detection of thyrotropin-releasing hormone based on azo coupling and surface-enhanced resonance Raman spectroscopy. Analyst, The, 2016, 141, 5181-5188.	1.7	13
168	Nanoscale pH Profile at a Solution/Solid Interface by Chemically Modified Tip-Enhanced Raman Scattering. Journal of Physical Chemistry C, 2016, 120, 14663-14668.	1.5	43
169	Far-ultraviolet spectroscopy of solid and liquid states: characteristics, instrumentation, and applications. Analyst, The, 2016, 141, 3962-3981.	1.7	29
170	Far―and Deepâ€UV Spectroscopy of Semiconductor Nanoparticles Measured Based on Attenuated Total Reflectance spectroscopy. ChemPhysChem, 2016, 17, 516-519.	1.0	22
171	Simple and rapid determination of free fatty acids in brown rice by FTIR spectroscopy in conjunction with a second-derivative treatment. Food Chemistry, 2016, 191, 7-11.	4.2	21
172	Absorption intensity changes and frequency shifts of fundamental and first overtone bands for OH stretching vibration of methanol upon methanol–pyridine complex formation in CCl ₄ : analysis by NIR/IR spectroscopy and DFT calculations. Physical Chemistry Chemical Physics, 2016, 18, 5580-5586.	1.3	20
173	Critical Review Upon the Role and Potential of Fluorescence and Near-Infrared Imaging and Absorption Spectroscopy in Cancer Related Cells, Serum, Saliva, Urine and Tissue Analysis. Current Medicinal Chemistry, 2016, 23, 3052-3077.	1.2	35
174	Analysis of Electronic Transition of Aqueous Solutions Studied by Far-ultraviolet Spectroscopy. Bunseki Kagaku, 2015, 64, 173-184.	0.1	0
175	Tip-Enhanced Raman Scattering of Nanomaterials. E-Journal of Surface Science and Nanotechnology, 2015, 13, 329-338.	0.1	2
176	Fabrication of a highly sensitive surface-enhanced Raman scattering substrate for monitoring the catalytic degradation of organic pollutants. Journal of Materials Chemistry A, 2015, 3, 13556-13562.	5.2	46
177	Nanoporous silver microstructure for single particle surface-enhanced Raman scattering spectroscopy. RSC Advances, 2015, 5, 1391-1397.	1.7	16
178	Developing dissolution testing methodologies for extended-release oral dosage forms with supersaturating properties. Case example: Solid dispersion matrix of indomethacin. International Journal of Pharmaceutics, 2015, 490, 368-374.	2.6	10
179	Different behaviour of molecules in dark SERS state on colloidal Ag nanoparticles estimated by truncated power law analysis of blinking SERS. Physical Chemistry Chemical Physics, 2015, 17, 21204-21210.	1.3	18
180	The effects of Au nanoparticle size (5–60 nm) and shape (sphere, rod, cube) over electronic states and photocatalytic activities of TiO ₂ studied by far- and deep-ultraviolet spectroscopy. RSC Advances, 2015, 5, 13648-13652.	1.7	33

#	Article	IF	CITATIONS
181	Anisotropic gold nanoassembly: a study on polarization-dependent and polarization-selective surface-enhanced Raman scattering. Physical Chemistry Chemical Physics, 2015, 17, 4268-4276.	1.3	15
182	Surface Effect of Alumina on the First Electronic Transition of Liquid Water Studied by Far-Ultraviolet Spectroscopy. Journal of Physical Chemistry Letters, 2015, 6, 1022-1026.	2.1	28
183	Raman Spectral Dynamics of Single Cells in the Early Stages of Growth Factor Stimulation. Biophysical Journal, 2015, 108, 2148-2157.	0.2	16
184	Semiconductor-enhanced Raman scattering for highly robust SERS sensing: the case of phosphate analysis. Chemical Communications, 2015, 51, 7641-7644.	2.2	56
185	Characterization of SiC-grown epitaxial graphene microislands using tip-enhanced Raman spectroscopy. Physical Chemistry Chemical Physics, 2015, 17, 28993-28999.	1.3	14
186	Intermolecular hydrogen bondings in the poly(3-hydroxybutyrate) and chitin blends: Their effects on the crystallization behavior and crystal structure of poly(3-hydroxybutyrate). Polymer, 2015, 75, 141-150.	1.8	45
187	Advances in Molecular Structure and Interaction Studies Using Near-Infrared Spectroscopy. Chemical Reviews, 2015, 115, 9707-9744.	23.0	189
188	Semiconductor-driven "turn-off―surface-enhanced Raman scattering spectroscopy: application in selective determination of chromium(<scp>vi</scp>) in water. Chemical Science, 2015, 6, 342-348.	3.7	92
189	Single-molecular surface-enhanced resonance Raman scattering as a quantitative probe of local electromagnetic field: The case of strong coupling between plasmonic and excitonic resonance. Physical Review B, 2014, 89, .	1.1	53
190	Enantioselective Discrimination of Alcohols by Hydrogen Bonding: A SERS Study. Angewandte Chemie - International Edition, 2014, 53, 13866-13870.	7.2	83
191	Concept and properties of an infrared hybrid single-beam spectrum and its application to eliminate solvent bands and other background interferences. Talanta, 2014, 119, 105-110.	2.9	4
192	Frequencies and absorption intensities of the fundamental and the first overtone of NH stretching vibrations of pyrroleacetylene and pyrroleethylene complexes studied by density-functional-theory calculation. Vibrational Spectroscopy, 2014, 72, 124-127.	1.2	15
193	Fundamental studies on enhancement and blinking mechanism of surface-enhanced Raman scattering (SERS) and basic applications of SERS biological sensing. Frontiers of Physics, 2014, 9, 31-46.	2.4	71
194	Consistent changes in electronic states and photocatalytic activities of metal (Au, Pd, Pt)-modified TiO ₂ studied by far-ultraviolet spectroscopy. Chemical Communications, 2014, 50, 2117-2119.	2.2	51
195	Recent progress and frontiers in the electromagnetic mechanism of surface-enhanced Raman scattering. Journal of Photochemistry and Photobiology C: Photochemistry Reviews, 2014, 21, 81-104.	5.6	131
196	Raman and Autofluorescence Spectrum Dynamics along the HRG-Induced Differentiation Pathway of MCF-7 Cells. Biophysical Journal, 2014, 107, 2221-2229.	0.2	19
197	Template free synthesis of dendritic silver nanostructures and their application in surface-enhanced Raman scattering. RSC Advances, 2014, 4, 52686-52689.	1.7	20
198	Tip-Enhanced Raman Scattering of the Local Nanostructure of Epitaxial Graphene Grown on 4H-SiC (0001ì). Journal of Physical Chemistry C, 2014, 118, 25809-25815.	1.5	42

#	Article	IF	CITATIONS
199	Significant enhancement of photocatalytic activity of rutile TiO ₂ compared with anatase TiO ₂ upon Pt nanoparticle deposition studied by far-ultraviolet spectroscopy. Physical Chemistry Chemical Physics, 2014, 16, 7749-7753.	1.3	40
200	Solvated States of Poly- <scp>l</scp> -alanine α-Helix Explored by Raman Optical Activity. Journal of Physical Chemistry A, 2014, 118, 3655-3662.	1.1	28
201	Rydberg and π–π* Transitions in Film Surfaces of Various Kinds of Nylons Studied by Attenuated Total Reflection Far-Ultraviolet Spectroscopy and Quantum Chemical Calculations: Peak Shifts in the Spectra and Their Relation to Nylon Structure and Hydrogen Bondings. Journal of Physical Chemistry B. 2014. 118. 11855-11861.	1.2	37
202	Study of the hydrogen bonding of 1,4-bis[(3,4,5-trihexyloxyphenyl)hydrazide]phenylene in crystalline and liquid crystalline phases using infrared, Raman, and two-dimensional correlation spectroscopy. Vibrational Spectroscopy, 2014, 73, 150-157.	1.2	4
203	Tip-enhanced Raman spectroscopic measurement of stress change in the local domain of epitaxial graphene on the carbon face of 4H-SiC(000–1). Physical Chemistry Chemical Physics, 2014, 16, 20236-20240.	1.3	28
204	Exploring the Effect of Intermolecular H-Bonding: A Study on Charge-Transfer Contribution to Surface-Enhanced Raman Scattering of <i>p</i> -Mercaptobenzoic Acid. Journal of Physical Chemistry C, 2014, 118, 10191-10197.	1.5	91
205	Contribution of hydrogen bonding to charge-transfer induced surface-enhanced Raman scattering of an intermolecular system comprising p-aminothiophenol and benzoic acid. Physical Chemistry Chemical Physics, 2014, 16, 3153.	1.3	49
206	Combined IR/NIR and Density Functional Theory Calculations Analysis of the Solvent Effects on Frequencies and Intensities of the Fundamental and Overtones of the Câ•O Stretching Vibrations of Acetone and 2-Hexanone. Journal of Physical Chemistry A, 2014, 118, 2576-2583.	1.1	40
207	Two-dimensional correlation infrared spectroscopy studies on the thermal-induced mesophase of 4-nitrobenzohydrazide derivative. Vibrational Spectroscopy, 2014, 70, 115-119.	1.2	4
208	Recent Progress of Near-Infrared (NIR) Imaging —Development of Novel Instruments and Their Applicability for Practical Situations—. Analytical Sciences, 2014, 30, 143-150.	0.8	30
209	Monitoring of Recrystallisation of Microcrystalline Cellulose inside Pharmaceutical Tablets during Storage Using near Infrared Diffuse Reflectance Spectroscopy. Journal of Near Infrared Spectroscopy, 2014, 22, 205-210.	0.8	5
210	Feasibility Study of Diffuse Reflectance and Transmittance near Infrared Spectroscopy for Rapid Analysis of Ascorbic Acid Concentration in Bilayer Tablets Using a High-Speed Polychromator-Type Spectrometer. Journal of Near Infrared Spectroscopy, 2014, 22, 189-197.	0.8	10
211	Spectroscopic approach for dynamic bioanalyte tracking with minimal concentration information. Scientific Reports, 2014, 4, 7013.	1.6	38
212	Design of an anti-aggregated SERS sensing platform for metal ion detection based on bovine serum albumin-mediated metal nanoparticles. Chemical Communications, 2013, 49, 7334.	2.2	22
213	Quantum Mechanical Interpretation of Intermolecular Vibrational Modes of Crystalline Poly-(<i>R</i>)-3-Hydroxybutyrate Observed in Low-Frequency Raman and Terahertz Spectra. Journal of Physical Chemistry B, 2013, 117, 2180-2187.	1.2	58
214	Terahertz Spectroscopy in Polymer Research: Assignment of Intermolecular Vibrational Modes and Structural Characterization of Poly(3-Hydroxybutyrate). IEEE Transactions on Terahertz Science and Technology, 2013, 3, 248-258.	2.0	55
215	Pulse Laser Photolysis of Aqueous Ozone in the Microsecond Range Studied by Time-Resolved Far-Ultraviolet Absorption Spectroscopy. Analytical Chemistry, 2013, 85, 4500-4506.	3.2	18
216	A study on the interaction of single-walled carbon nanotubes (SWCNTs) and polystyrene (PS) at the interface in SWCNT–PS nanocomposites using tip-enhanced Raman spectroscopy. Physical Chemistry Chemical Physics, 2013, 15, 20618.	1.3	40

#	Article	IF	CITATIONS
217	Surface-Enhanced Phosphorescence Measurement by an Optically Trapped Colloidal Ag Nanoaggregate on Anionic Thiacarbocyanine H-Aggregate. Journal of Physical Chemistry C, 2013, 117, 2460-2466.	1.5	3
218	Brill transition of nylon-6 characterized by low-frequency vibration through terahertz absorption spectroscopy. Chemical Physics Letters, 2013, 575, 36-39.	1.2	28
219	Pressure-induced variation of cellulose tablet studied by two-dimensional (2D) near-infrared (NIR) correlation spectroscopy in conjunction with projection pretreatment. Vibrational Spectroscopy, 2013, 65, 28-35.	1.2	30
220	Characterization of adsorption mode of new B ₂ bradykinin receptor antagonists onto colloidal Ag substrate. Journal of Raman Spectroscopy, 2013, 44, 212-218.	1.2	9
221	Adsorption mode of neurotensin family peptides onto a colloidal silver surface: SERS studies. Journal of Raman Spectroscopy, 2013, 44, 355-361.	1.2	7
222	Tip-Enhanced Raman Spectroscopy Study of Local Interactions at the Interface of Styrene–Butadiene Rubber/Multiwalled Carbon Nanotube Nanocomposites. Journal of Physical Chemistry C, 2013, 117, 1436-1440.	1.5	39
223	Molecular structure and hydrogen bonding in pure liquid ethylene glycol and ethylene glycol–water mixtures studied using NIR spectroscopy. Physical Chemistry Chemical Physics, 2013, 15, 18694.	1.3	68
224	Truncated Power Law Analysis of Blinking SERS of Thiacyanine Molecules Adsorbed on Single Silver Nanoaggregates by Excitation at Various Wavelengths. Journal of Physical Chemistry C, 2013, 117, 9397-9403.	1.5	17
225	Electronic Transitions of Protonated and Deprotonated Amino Acids in Aqueous Solution in the Region 145–300 nm Studied by Attenuated Total Reflection Far-Ultraviolet Spectroscopy. Journal of Physical Chemistry A, 2013, 117, 2517-2528.	1.1	39
226	Application of a newly developed portable NIR imaging device to monitor the dissolution process of tablets. Analytical and Bioanalytical Chemistry, 2013, 405, 9401-9409.	1.9	40
227	Influence of backbone length and synthetic mutations on orientation of neurotensin fragments adsorbed onto a colloidal silver surface: SERS studies. Journal of Raman Spectroscopy, 2013, 44, 55-62.	1.2	4
228	Excitation laser energy dependence of surface-enhanced fluorescence showing plasmon-induced ultrafast electronic dynamics in dye molecules. Physical Review B, 2013, 87, .	1.1	39
229	Terahertz vibrational spectroscopy of poly(3-hydroxybutyrate) and nylon: Potential of terahertz spectroscopy for polymer science. , 2013, , .		1
230	Electronic transitions in liquid amides studied by using attenuated total reflection far-ultraviolet spectroscopy and quantum chemical calculations. Journal of Chemical Physics, 2013, 139, 154301.	1.2	41
231	Multiple-Perturbation Two-Dimensional Near-Infrared Correlation Study of Time-Dependent Water Absorption Behavior of Cellulose Affected by Pressure. Applied Spectroscopy, 2013, 67, 163-170.	1.2	25
232	Development of a time-resolved attenuated total reflectance spectrometer in far-ultraviolet region. Review of Scientific Instruments, 2012, 83, 073103.	0.6	21
233	Far-Ultraviolet Spectroscopy in the Solid and Liquid States: A Review. Applied Spectroscopy, 2012, 66, 1-25.	1.2	77
234	Development of a Near-Infrared/Mid-Infrared Dual-Region Spectrometer for Online Process Analysis. Applied Spectroscopy, 2012, 66, 773-781.	1.2	17

#	Article	IF	CITATIONS
235	Development of Far-UV Spectroscopy for Liquid and Solid and Its Application to Analytical Chemistry. Bunseki Kagaku, 2012, 61, 591-603.	0.1	3
236	Development of a Flexible Fiber Surface-Enhanced Raman Scattering (SERS) Probe Using a Hollow Optical Fiber and Gold Nanoparticles. Applied Spectroscopy, 2012, 66, 1022-1026.	1.2	7
237	A Feasibility Study on Non-Destructive Determination of Oil Content in Palm Fruits by Visible–Near Infrared Spectroscopy. Journal of Near Infrared Spectroscopy, 2012, 20, 687-694.	0.8	16
238	Near-Infrared Spectroscopy—Its Versatility in Analytical Chemistry. Analytical Sciences, 2012, 28, 545-563.	0.8	222
239	Biological Applications of SERS Using Functional Nanoparticles. ACS Symposium Series, 2012, , 181-234.	0.5	7
240	pH-Dependent SERS by Semiconductor-Controlled Charge-Transfer Contribution. Journal of Physical Chemistry C, 2012, 116, 24829-24836.	1.5	32
241	The effect of metal cations on the nature of the first electronic transition of liquid water as studied by attenuated total reflection far-ultraviolet spectroscopy. Physical Chemistry Chemical Physics, 2012, 14, 8097.	1.3	44
242	Elucidating Electronic Transitions from Ïf Orbitals of Liquid <i>n-</i> and Branched Alkanes by Far-Ultraviolet Spectroscopy and Quantum Chemical Calculations. Journal of Physical Chemistry A, 2012, 116, 11957-11964.	1.1	51
243	Compression effect on sustained-release and water absorption properties of cellulose tablets studied by heterospectral two-dimensional (2D) correlation analysis. Analytical Methods, 2012, 4, 1530-1537.	1.3	16
244	Sequential Identification of Model Parameters by Derivative Double Two-Dimensional Correlation Spectroscopy and Calibration-Free Approach for Chemical Reaction Systems. Analytical Chemistry, 2012, 84, 8330-8339.	3.2	13
245	Effects of Lanthanoid Cations on the First Electronic Transition of Liquid Water Studied Using Attenuated Total Reflection Far-Ultraviolet Spectroscopy: Ligand Field Splitting of Lanthanoid Hydrates in Aqueous Solutions. Inorganic Chemistry, 2012, 51, 10650-10656.	1.9	25
246	pH-Response Mechanism of <i>p</i> -Aminobenzenethiol on Ag Nanoparticles Revealed By Two-Dimensional Correlation Surface-Enhanced Raman Scattering Spectroscopy. Journal of Physical Chemistry Letters, 2012, 3, 3204-3209.	2.1	60
247	The dielectric constant dependence of absorption intensities and wavenumbers of the fundamental and overtone transitions of stretching vibration of the hydrogen fluoride studied by quantum chemistry calculations. Journal of Molecular Structure, 2012, 1018, 102-106.	1.8	20
248	Generation of Pronounced Resonance Profile of Charge-Transfer Contributions to Surface-Enhanced Raman Scattering. Journal of Physical Chemistry C, 2012, 116, 2515-2520.	1.5	32
249	Effects of Molar Mass of Poly(l-lactide acid) on the Crystallization of Poly[(R)-3-hydroxybutyrate] in Their Ultrathin Blend Films. Macromolecules, 2012, 45, 2485-2493.	2.2	22
250	Simultaneous Synchrotron SAXS/WAXD Study of Composition Fluctuations, Cold-Crystallization, and Melting in Biodegradable Polymer Blends of Cellulose Acetate Butyrate and Poly(3-hydroxybutyrate). Macromolecules, 2012, 45, 2783-2795.	2.2	24
251	Isothermal crystallization of poly(3-hydroxybutyrate) studied by terahertz two-dimensional correlation spectroscopy. Applied Physics Letters, 2012, 100, .	1.5	38
252	Labelâ€free detection of binary mixtures of proteins using surfaceâ€enhanced Raman scattering. Journal of Raman Spectroscopy, 2012, 43, 706-711.	1.2	26

#	Article	IF	CITATIONS
253	Inhibition Assay of Yeast Cell Walls by Plasmon Resonance Rayleigh Scattering and Surface-Enhanced Raman Scattering Imaging. Langmuir, 2012, 28, 8952-8958.	1.6	19
254	Power-law analysis of surface-plasmon-enhanced electromagnetic field dependence of blinking SERS of thiacyanine or thiacarbocyanine adsorbed on single silver nanoaggregates. Physical Chemistry Chemical Physics, 2011, 13, 7439.	1.3	24
255	Analysis of excitation laser intensity dependence of blinking SERRS of thiacarbocyanine adsorbed on single silver nanoaggregates by using a power law with an exponential function. Chemical Communications, 2011, 47, 3888.	2.2	13
256	Solid-State Low Temperature → Middle Temperature Phase Transition of Linoleic Acid Studied by FTIR Spectroscopy. Journal of Physical Chemistry B, 2011, 115, 6289-6295.	1.2	17
257	Study on the Phase Transition Behavior of Poly(butylene adipate) in its Blends with Poly(vinyl phenol). Journal of Physical Chemistry B, 2011, 115, 1950-1957.	1.2	41
258	Low- <i>n</i> Rydberg Transitions of Liquid Ketones Studied by Attenuated Total Reflection Far-Ultraviolet Spectroscopy. Journal of Physical Chemistry A, 2011, 115, 562-568.	1.1	50
259	Polarization and temperature dependent spectra of poly(3-hydroxyalkanoate)s measured at terahertz frequencies. Physical Chemistry Chemical Physics, 2011, 13, 9173.	1.3	97
260	Solvent Dependence of Absorption Intensities and Wavenumbers of the Fundamental and First Overtone of NH Stretching Vibration of Pyrrole Studied by Near-Infrared/Infrared Spectroscopy and DFT Calculations. Journal of Physical Chemistry A, 2011, 115, 1194-1198.	1.1	48
261	Hydrogen Bonding Effects on the Wavenumbers and Absorption Intensities of the OH Fundamental and the First, Second, and Third Overtones of Phenol and 2,6-Dihalogenated Phenols Studied by Visible/Near-Infrared/Infrared Spectroscopy. Journal of Physical Chemistry A, 2011, 115, 9845-9853.	1.1	60
262	Thermally Induced Exchanges of Hydrogen Bonding Interactions and Their Effects on Phase Structures of Poly(3-hydroxybutyrate) and Poly(4-vinylphenol) Blends. Macromolecules, 2011, 44, 2229-2239.	2.2	31
263	Infrared Spectroscopy and X-ray Diffraction Studies of Thermal Behavior and Lamella Structures of Poly(3-hydroxybutyrate- <i>co</i> -3-hydroxyvalerate) (P(HB- <i>co</i> -HV)) with PHB-Type Crystal Structure. Macromolecules, 2011, 44, 2829-2837.	2.2	44
264	Far-Ultraviolet Spectra of <i>n</i> -Alkanes and Branched Alkanes in the Liquid Phase Observed Using an Attenuated Total Reflection—Far Ultraviolet (ATR-FUV) Spectrometer. Applied Spectroscopy, 2011, 65, 221-226.	1.2	47
265	Asynchronous Orthogonal Sample Design Scheme for TwoDimensional Correlation Spectroscopy (2D-COS) and Its Application in Probing Intermolecular Interactions from Overlapping Infrared (IR) Bands. Applied Spectroscopy, 2011, 65, 901-917.	1.2	42
266	Compression-Induced Morphological and Molecular Structural Changes of Cellulose Tablets Probed with near Infrared Imaging. Journal of Near Infrared Spectroscopy, 2011, 19, 15-22.	0.8	23
267	Analysis of Water and Aqueous Solutions by Far Ultraviolet Spectroscopy. Bunseki Kagaku, 2011, 60, 19-31.	0.1	2
268	A study on the crystallization behavior of poly(β-hydroxybutyrate) thin films on Si wafers. Polymer, 2011, 52, 3865-3870.	1.8	44
269	Selective SERS detection of each polycyclic aromatic hydrocarbon (PAH) in a mixture of five kinds of PAHs. Journal of Raman Spectroscopy, 2011, 42, 945-950.	1.2	63
270	Experimental parameters for the SERS of nitrate ion for labelâ€free semiâ€quantitative detection of proteins and mechanism for proteins to form SERS hot sites: a SERS study. Journal of Raman Spectroscopy, 2011, 42, 1713-1721.	1.2	26

#	Article	IF	CITATIONS
271	Intermolecular interactions and crystallization behaviors of biodegradable polymer blends between poly (3-hydroxybutyrate) and cellulose acetate butyrate studied by DSC, FT-IR, and WAXD. Polymer, 2011, 52, 461-471.	1.8	51
272	Near Infrared Quantitative Analysis of Total Curcuminoids in Rhizomes of <i>Curcuma Longa</i> by Moving Window Partial Least Squares Regression. Journal of Near Infrared Spectroscopy, 2010, 18, 263-269.	0.8	12
273	Siteâ€specific deposition of Ag nanoparticles on ZnO nanorod arrays via galvanic reduction and their SERS applications. Journal of Raman Spectroscopy, 2010, 41, 907-913.	1.2	54
274	Difference in time dependence of surface-enhanced Raman scattering spectra of thiacarbocyanine J- and H-aggregates adsorbed on single silver nanoaggregates. Chemical Physics Letters, 2010, 493, 309-313.	1.2	12
275	Quantitative evaluation of electromagnetic enhancement in surface-enhanced resonance Raman scattering from plasmonic properties and morphologies of individual Ag nanostructures. Physical Review B, 2010, 81, .	1.1	152
276	Blinking SERS from Single Ag Nanoaggregates with Various LSPR Wavelengths. , 2010, , .		0
277	Blinking of SERRS Excited by Various Laser Intensities. , 2010, , .		0
278	PLLA Mesophase and Its Phase Transition Behavior in the PLLAâ^'PEGâ^'PLLA Copolymer As Revealed by Infrared Spectroscopy. Macromolecules, 2010, 43, 4240-4246.	2.2	111
279	Higher order conformation of poly(3-hydroxyalkanoates) studied by terahertz time-domain spectroscopy. Applied Physics Letters, 2010, 96, .	1.5	70
280	FTIR Study on Hydrogen-Bonding Interactions in Biodegradable Polymer Blends of Poly(3-hydroxybutyrate) and Poly(4-vinylphenol). Macromolecules, 2010, 43, 3897-3902.	2.2	125
281	Sensing of polycyclic aromatic hydrocarbons with cyclodextrin inclusion complexes on silver nanoparticles by surface-enhanced Raman scattering. Analyst, The, 2010, 135, 1389.	1.7	118
282	Effect of Cations on Absorption Bands of First Electronic Transition of Liquid Water. Journal of Physical Chemistry A, 2010, 114, 8319-8322.	1.1	55
283	Highly Sensitive Protein Concentration Assay over a Wide Range via Surface-Enhanced Raman Scattering of Coomassie Brilliant Blue. Analytical Chemistry, 2010, 82, 4325-4328.	3.2	58
284	Power-law statistics in blinking SERS of thiacyanine adsorbed on a single silver nanoaggregate. Physical Chemistry Chemical Physics, 2010, 12, 7457.	1.3	27
285	Experimental evaluation of the twofold electromagnetic enhancement theory of surface-enhanced resonance Raman scattering. Physical Review B, 2009, 79, .	1.1	75
286	Spectral shapes of surface-enhanced resonance Raman scattering sensitive to the refractive index of media around single Ag nanoaggregates. Applied Physics Letters, 2009, 95, .	1.5	24
287	<i>In situ</i> nucleation and growth of silver nanoparticles in membrane materials: a controllable roughened SERS substrate with high reproducibility. Journal of Raman Spectroscopy, 2009, 40, 31-37.	1.2	33
288	Multivariate data analysis for Raman spectroscopic imaging. Journal of Raman Spectroscopy, 2009, 40, 1720-1725.	1.2	96

#	Article	IF	CITATIONS
289	Frequencies and absorption intensities of fundamentals and overtones of NH stretching vibrations of pyrrole and pyrrole–pyridine complex studied by near-infrared/infrared spectroscopy and density-functional-theory calculations. Chemical Physics Letters, 2009, 482, 320-324.	1.2	43
290	Surface-enhanced Raman scattering for protein detection. Analytical and Bioanalytical Chemistry, 2009, 394, 1719-1727.	1.9	317
291	Surface-enhanced Raman scattering: realization of localized surface plasmon resonance using unique substrates and methods. Analytical and Bioanalytical Chemistry, 2009, 394, 1747-1760.	1.9	107
292	Specific crystal structure of poly(3-hydroxybutyrate) thin films studied by infrared reflection–absorption spectroscopy. Vibrational Spectroscopy, 2009, 51, 132-135.	1.2	21
293	Attenuated total reflectance–far ultraviolet (ATR–FUV) spectra of CH3OH, CH3OD, CD3OH and CD3OD in a liquid phase â^¼Rydberg statesâ^¼. Chemical Physics Letters, 2009, 476, 205-208.	1.2	58
294	Surface Plasmon Excitation and Surface-Enhanced Raman Scattering Using Two-Dimensionally Close-Packed Gold Nanoparticles. Journal of Physical Chemistry C, 2009, 113, 11689-11694.	1.5	24
295	A novel reversed reporting agent method for surface-enhanced Raman scattering; highly sensitive detection of glutathione in aqueous solutions. Analyst, The, 2009, 134, 2468.	1.7	45
296	Characteristics of surface-enhanced Raman scattering and surface-enhanced fluorescence using a single and a double layer gold nanostructure. Physical Chemistry Chemical Physics, 2009, 11, 7484.	1.3	22
297	Double Orthogonal Sample Design Scheme and Corresponding Basic Patterns in Two-Dimensional Correlation Spectra for Probing Subtle Spectral Variations Caused by Intermolecular Interactions. Journal of Physical Chemistry A, 2009, 113, 12142-12156.	1.1	34
298	SPR and SERS characteristics of gold nanoaggregates withÂdifferent morphologies. Applied Physics B: Lasers and Optics, 2008, 93, 165-170.	1.1	38
299	Preparation and SERS study of triangular silver nanoparticle selfâ€assembled films. Journal of Raman Spectroscopy, 2008, 39, 1673-1678.	1.2	39
300	Crystallization behavior of poly(l-lactic acid) affected by the addition of a small amount of poly(3-hydroxybutyrate). Polymer, 2008, 49, 4204-4210.	1.8	73
301	Perturbation-correlation moving-window 2D correlation analysis of temperature-dependent infrared spectra of a poly(vinyl alcohol) film. Journal of Molecular Structure, 2008, 883-884, 181-186.	1.8	35
302	Crystal Structures, Thermal Behaviors, and Câ^'H···Oâ•€ Hydrogen Bondings of Poly(3-hydroxyvalerate) and Poly(3-hydroxybutyrate) Studied by Infrared Spectroscopy and X-ray Diffraction. Macromolecules, 2008, 41, 4305-4312.	2.2	85
303	Potential of Far-Ultraviolet Absorption Spectroscopy as a Highly Sensitive Analysis Method for Aqueous Solutions. Part II: Monitoring the Quality of Semiconductor Wafer Cleaning Solutions Using Attenuated Total Reflection. Applied Spectroscopy, 2008, 62, 1022-1027.	1.2	22
304	Crystalline Lamellae and Surface Morphology of Biodegradable Polyhydroxyalkanoate Thin Films: Thermal Behavior and Comparison between Poly(3-hydroxybutyrate- <i>co</i> -3-hydroxyhexanoate) and Poly(3-hydroxybutyrate). Macromolecules, 2008, 41, 1713-1719.	2.2	20
305	Melt Crystallization and Crystal Transition of Poly(butylene adipate) Revealed by Infrared Spectroscopy. Journal of Physical Chemistry B, 2008, 112, 3311-3314.	1.2	56
306	Direct observation of the absorption bands of the first electronic transition in liquid H2O and D2O by attenuated total reflectance far-UV spectroscopy. Journal of Chemical Physics, 2008, 129, 234510.	1.2	79

#	Article	IF	CITATIONS
307	An attenuated total reflectance far-UV spectrometer. Review of Scientific Instruments, 2007, 78, 103107.	0.6	73
308	Second enhancement in surface-enhanced resonance Raman scattering revealed by an analysis of anti-Stokes and Stokes Raman spectra. Physical Review B, 2007, 76, .	1.1	112
309	Comparison of miscibility and structure of poly(3-hydroxybutyrate-co-3-hydroxyhexanoate)/poly(I-lactic acid) blends with those of poly(3-hydroxybutyrate)/poly(I-lactic acid) blends studied by wide angle X-ray diffraction, differential scanning calorimetry, and FTIR microspectroscopy, Polymer, 2007, 48, 1749-1755.	1.8	87
310	Formation and stability of Î ² -structure in biodegradable ultra-high-molecular-weight poly(3-hydroxybutyrate) by infrared, Raman, andÂquantum chemical calculation studies. Polymer, 2007, 48, 2672-2680.	1.8	44
311	Study on multimers and their structures in molecular association mixture. Science in China Series B: Chemistry, 2007, 50, 23-31.	0.8	3
312	A Non-Destructive Method for Assessing Interior and Surface Hair Damage by Near Infrared Spectroscopy. Journal of Society of Cosmetic Chemists of Japan, 2007, 41, 22-30.	0.0	0
313	Câ^'H···OC Hydrogen Bonding and Isothermal Crystallization Kinetics of Poly(3-hydroxybutyrate) Investigated by Near-Infrared Spectroscopy. Macromolecules, 2006, 39, 3841-3847.	2.2	64
314	Crystal and Lamella Structure and Câ^'H··ÔC Hydrogen Bonding of Poly(3-hydroxyalkanoate) Studied by X-ray Diffraction and Infrared Spectroscopy. Macromolecules, 2006, 39, 1525-1531.	2.2	109
315	Orientation of Merocyanine Dye in Mixed Langmuir-Blodgett Films Investigated by Visible Absorption Spectroscopy. Molecular Crystals and Liquid Crystals, 2006, 445, 93/[383]-99/[389].	0.4	6
316	Crystallization Behaviors of Poly(3-hydroxybutyrate) and Poly(l-lactic acid) in Their Immiscible and Miscible Blends. Journal of Physical Chemistry B, 2006, 110, 24463-24471.	1.2	79
317	Multi-Objective Genetic Algorithm-Based Sample Selection for Partial Least Squares Model Building with Applications to Near-Infrared Spectroscopic Data. Applied Spectroscopy, 2006, 60, 631-640.	1.2	10
318	Sampling Techniques. , 2006, , 133-143.		0
319	Latent-Variable Analysis of Multivariate Data in Infrared Spectrometry. , 2006, , 145-162.		0
320	X-ray diffraction and infrared spectroscopy studies on crystal and lamellar structure and cho hydrogen bonding of biodegradable poly(hydroxyalkanoate). Macromolecular Research, 2006, 14, 408-415.	1.0	27
321	Raman microspectroscopy study of structure, dispersibility, and crystallinity of poly(hydroxybutyrate)/poly(l-lactic acid) blends. Polymer, 2006, 47, 3132-3140.	1.8	86
322	Investigations of bagged kernel partial least squares (KPLS) and boosting KPLS with applications to near-infrared (NIR) spectra. Journal of Chemometrics, 2006, 20, 436-444.	0.7	40
323	Other Topics. , 2006, , 341-399.		0
324	Surface-enhanced resonance Raman scattering and background light emission coupled with plasmon of single Ag nanoaggregates. Journal of Chemical Physics, 2006, 124, 134708.	1.2	103

#	Article	IF	CITATIONS
325	Hyper-Rayleigh scattering and hyper-Raman scattering of dye-adsorbed silver nanoparticles induced by a focused continuous-wave near-infrared laser. Applied Physics Letters, 2006, 88, 084102.	1.5	53
326	Applications to Foodstuffs. , 2006, , 279-340.		0
327	Principles of Molecular Vibrations for Near-Infrared Spectroscopy. , 2006, , 11-46.		10
328	Applications to Agricultural and Marine Products. , 2006, , 163-277.		7
329	Optimisation of Prediction Performance Using Region Orthogonal Signal Correction. NIR News, 2006, 17, 14-15.	1.6	0
330	New Wavelength Selection Methods: Part 1. NIR News, 2005, 16, 10-11.	1.6	2
331	New Wavelength Selection Methods: Part 2. NIR News, 2005, 16, 6-8.	1.6	1
332	Structure, Dispersibility, and Crystallinity of Poly(hydroxybutyrate)/Poly(l-lactic acid) Blends Studied by FT-IR Microspectroscopy and Differential Scanning Calorimetry. Macromolecules, 2005, 38, 6445-6454.	2.2	233
333	Conformation Rearrangement and Molecular Dynamics of Poly(3-hydroxybutyrate) during the Melt-Crystallization Process Investigated by Infrared and Two-Dimensional Infrared Correlation Spectroscopy. Macromolecules, 2005, 38, 4274-4281.	2.2	120
334	Changes in excitation profiles of surface-enhanced resonance Raman scattering induced by changes in surface plasmon resonance of single Ag nano-aggregates. Chemical Physics Letters, 2004, 389, 225-229.	1.2	39
335	Thermal phase behavior of triethylamine–water mixtures studied by near-infrared spectroscopy: band shift of the first overtone of the C–H stretching modes and the phase diagram. Chemical Physics Letters, 2004, 393, 403-408.	1.2	30
336	Premelting Behavior of a Langmuirâ^Blodgett Film of Dioctadecyldimethylammonium-Au(dmit)2Salt. Journal of Physical Chemistry B, 2004, 108, 19354-19360.	1.2	8
337	Structural Changes and Crystallization Dynamics of Poly(l-lactide) during the Cold-Crystallization Process Investigated by Infrared and Two-Dimensional Infrared Correlation Spectroscopy. Macromolecules, 2004, 37, 6433-6439.	2.2	257
338	Self-Assembled Metal Colloid Films:  Two Approaches for Preparing New SERS Active Substrates. Langmuir, 2004, 20, 1298-1304.	1.6	146
339	Thermal Behavior and Molecular Interaction of Poly(3-hydroxybutyrate-co-3-hydroxyhexanoate) Studied by Wide-Angle X-ray Diffraction. Macromolecules, 2004, 37, 3763-3769.	2.2	172
340	Infrared Spectroscopy Studies of CH···O Hydrogen Bondings and Thermal Behavior of Biodegradable Poly(hydroxyalkanoate). Macromolecules, 2004, 37, 7203-7213.	2.2	221
341	Weak Intermolecular Interactions during the Melt Crystallization of Poly(l-lactide) Investigated by Two-Dimensional Infrared Correlation Spectroscopy. Journal of Physical Chemistry B, 2004, 108, 11514-11520.	1.2	173
342	Relationship between the coil-globule transition of an aqueous poly(N-isopropylacrylamide) solution and structural changes in local conformations of the polymer. Macromolecular Symposia, 2004, 205, 209-224.	0.4	31

#	Article	IF	CITATIONS
343	Resolution of two-way data from spectroscopic monitoring of reaction or process systems by parallel vector analysis (PVA) and window factor analysis (WFA): inspection of the effect of mass balance, methods and simulations. Journal of Chemometrics, 2003, 17, 186-197.	0.7	38
344	Discrimination of various poly(propylene) copolymers and prediction of their ethylene content by near-infrared and Raman spectroscopy in combination with chemometric methods. Journal of Applied Polymer Science, 2003, 87, 616-625.	1.3	31
345	Potentials of variable–variable and sample–sample, generalized and statistical, two-dimensional correlation spectroscopies in investigations of chemical reactions. Chemometrics and Intelligent Laboratory Systems, 2003, 65, 1-15.	1.8	14
346	Direct demonstration for changes in surface plasmon resonance induced by surface-enhanced Raman scattering quenching of dye molecules adsorbed on single Ag nanoparticles. Applied Physics Letters, 2003, 83, 5557-5559.	1.5	57
347	Method based on polarized infrared spectroscopy for the determination of the spatial orientation of transition dipole moments of a ferroelectric liquid crystal. Applied Physics Letters, 2003, 83, 389-391.	1.5	1
348	Self-modeling curve resolution analysis of on-line vibrational spectra of polymerisation and transesterification. Macromolecular Symposia, 2002, 184, 229-248.	0.4	4
349	Conformational Change of Poly(N-isopropylacrylamide) during the Coilâ [~] Globule Transition Investigated by Attenuated Total Reflection/Infrared Spectroscopy and Density Functional Theory Calculation. Journal of Physical Chemistry A, 2002, 106, 3429-3435.	1.1	230
350	Comparison of Wavelets and Smoothing for Denoising Spectra for Two-Dimensional Correlation Spectroscopy. Applied Spectroscopy, 2002, 56, 1462-1469.	1.2	36
351	Self-Modeling Curve Resolution Study of Temperature-Dependent Near-Infrared Spectra of Water and the Investigation of Water Structure. Journal of Physical Chemistry A, 2002, 106, 760-766.	1.1	92
352	SELF-MODELING CURVE RESOLUTION (SMCR): PRINCIPLES, TECHNIQUES, AND APPLICATIONS. Applied Spectroscopy Reviews, 2002, 37, 321-345.	3.4	74
353	Title is missing!. Subsurface Sensing Technologies and Applications, 2002, 3, 19-34.	0.9	6
354	Short-Wave Near-Infrared Spectroscopy of Biological Fluids. 1. Quantitative Analysis of Fat, Protein, and Lactose in Raw Milk by Partial Least-Squares Regression and Band Assignment. Analytical Chemistry, 2001, 73, 64-71.	3.2	195
355	Sampleâ^'Sample and Wavenumberâ^'Wavenumber Two-Dimensional Correlation Analyses of Attenuated Total Reflection Infrared Spectra of Polycondensation Reaction of Bis(Hydroxyethyl terephthalate). Analytical Chemistry, 2001, 73, 5184-5190.	3.2	40
356	Studies on the Structure of Water Using Two-Dimensional Near-Infrared Correlation Spectroscopy and Principal Component Analysis. Analytical Chemistry, 2001, 73, 3153-3161.	3.2	281
357	Two-Dimensional Infrared Spectroscopy and Principle Component Analysis Studies of the Secondary Structure and Kinetics of Hydrogenâ "Deuterium Exchange of Human Serum Albumin. Journal of Physical Chemistry B, 2001, 105, 6251-6259.	1.2	74
358	Two-Dimensional/Attenuated Total Reflection Infrared Correlation Spectroscopy Studies on Secondary Structural Changes in Human Serum Albumin in Aqueous Solutions: pH-Dependent Structural Changes in the Secondary Structures and in the Hydrogen Bondings of Side Chains. Journal of Physical Chemistry B, 2001, 105, 4763-4769.	1.2	68
359	Polarized infrared spectroscopic study on changes in molecular orientation and interaction during phase transitions of a ferroelectric liquid crystal with a naphthalene ring. Liquid Crystals, 2001, 28, 327-331.	0.9	8
360	End-group characterization of homo- and copolyesters of cyclohexane-1,4-dimethanol. Journal of Polymer Science Part A, 2001, 39, 665-674.	2.5	23

#	Article	IF	CITATIONS
361	Fourier-Transform Raman Spectroscopic On-Line Monitoring of the Anionic Dispersion Block Copolymerization of Styrene and 1,3-Butadiene. Macromolecular Rapid Communications, 2001, 22, 690-693.	2.0	16
362	Two-dimensional infrared correlation spectroscopy studies of polymer blends 1: Chain conformation and bonding in atactic polystyrene-poly(2,6-dimethyl-1,4-phenylene ether) blends. AIP Conference Proceedings, 2000, , .	0.3	0
363	Two-dimensional Fourier-transform-Raman and near-infrared correlation spectroscopy studies of poly(methyl methacrylate) blends. Vibrational Spectroscopy, 2000, 23, 207-218.	1.2	38
364	Two-dimensional Raman-near infrared heterospectral correlation spectroscopy studies of the specific interactions in partially miscible blends of poly(methyl methacrylate) and poly(4-vinylphenol). AIP Conference Proceedings, 2000, , .	0.3	1
365	Generalized Two-Dimensional Correlation Spectroscopy. Applied Spectroscopy, 2000, 54, 236A-248A.	1.2	752
366	Two-Dimensional Near-Infrared Spectroscopy Study of Human Serum Albumin in Aqueous Solutions:Â Using Overtones and Combination Modes to Monitor Temperature-Dependent Changes in the Secondary Structure. Journal of Physical Chemistry B, 2000, 104, 5840-5847.	1.2	87
367	An Infrared Spectroscopy Study on Molecular Orientation and Structure in Mixed Langmuirâ^Blodgett Films of 2-Octadecyl-7,7,8,8-tetracyanoquinodimethane and Deuterated Stearic Acid:A Phase Separation and Freezing-in Effects of the Fatty Acid Domains. Langmuir, 2000, 16, 5142-5147.	1.6	12
368	A polarized infrared spectroscopic study on electric-field-induced layer rotation of ferroelectric liquid crystal mixtures with ultrashort pitch. Physical Chemistry Chemical Physics, 2000, 2, 3037-3042.	1.3	5
369	A New Possibility of the Generalized Two-Dimensional Correlation Spectroscopy. 2. Sampleâ^'Sample and Wavenumberâ^'Wavenumber Correlations of Temperature-Dependent Near-Infrared Spectra of Oleic Acid in the Pure Liquid State. Journal of Physical Chemistry A, 2000, 104, 6388-6394.	1.1	63
370	A New Possibility of the Generalized Two-Dimensional Correlation Spectroscopy. 1. Sampleâ^'Sample Correlation Spectroscopy. Journal of Physical Chemistry A, 2000, 104, 6380-6387.	1.1	105
371	Earlier Response of Carbonyl Groups in Electric-Field-Induced Dynamics of a Ferroelectric Liquid Crystal with a Naphthalene Ring Studied by Submicrosecond Multichannel Asynchronous Time-Resolved FT-IR Spectroscopy. Journal of Physical Chemistry B, 2000, 104, 7881-7884.	1.2	8
372	Resolution Enhancement and Band Assignments for the First Overtone of OH(D) Stretching Modes of Butanols by Two-Dimensional Near-Infrared Correlation Spectroscopy. 3. Thermal Dynamics of Hydrogen Bonding in Butan-1-(ol-d) and 2-Methylpropan-2-(ol-d) in the Pure Liquid States. Journal of Physical Chemistry A, 2000, 104, 4906-4911.	1.1	47
373	Potential of Raman Spectroscopy in Nondestructive Analysis of Foods. Japan Journal of Food Engineering, 2000, 1, 31-37.	0.1	2
374	Laser Spectral Analysis of Biomedical Materials-Functional Diagnosis by Laser Spectroscopy and New Spectral Analysis Methods The Review of Laser Engineering, 2000, 28, 271-280.	0.0	2
375	The temperature-induced changes in hydrogen bonding of decan-1-ol in the pure liquid phase studied by two-dimensional Fourier transform near-infrared correlation spectroscopy. Physical Chemistry Chemical Physics, 1999, 1, 797-800.	1.3	31
376	Studies on Control of Molecular Re-Arrangement in Langmuir-Blodgett Films of 2-Pentadecyl-7,7,8,8-Tetracyanoquinodimethane by Infrared and Ultraviolet-Visible Spectroscopy. Molecular Crystals and Liquid Crystals, 1999, 337, 321-324.	0.3	0
377	Thermal Stability of 1-Layer LB Film of Trichloro(Octadecyl)Silane. Molecular Crystals and Liquid Crystals, 1999, 337, 113-116.	0.3	4
378	The Effects of pH and Ionic Strength on the Aggregation of Bacteriochlorophyll c in Aqueous Organic Media: The Possibility of Two Kinds of Aggregates. Photochemistry and Photobiology, 1999, 70, 760-765.	1.3	14

#	Article	IF	CITATIONS
379	Structural Characterization of Langmuirâ^'Blodgett Films of Octadecyldimethylamine Oxide and Dioctadecyldimethylammonium Chloride. 2. Thickness Dependence of Thermal Behavior Investigated by Infrared Spectroscopy and Wetting Measurements. Langmuir, 1999, 15, 3601-3607.	1.6	25
380	Structural Characterization of Langmuirâ^'Blodgett Films of Octadecyldimethylamine Oxide and Dioctadecyldimethylammonium Chloride. 1. Reorientation of Molecular Assemblies during the Accumulation of Upper Layers Studied by Infrared Spectroscopy. Langmuir, 1999, 15, 3595-3600.	1.6	10
381	Analysis of Near-Infrared Spectra of Complicated Biological Fluids by Two-Dimensional Correlation Spectroscopy: Protein and Fat Concentration-Dependent Spectral Changes of Milk. Applied Spectroscopy, 1999, 53, 1582-1594.	1.2	82
382	Non-Destructive Analysis of Photo-Degradation of Poly(Methyl Methacrylate) by near Infrared Light-Fibre Spectroscopy and Chemometrics. Journal of Near Infrared Spectroscopy, 1999, 7, 27-32.	0.8	7
383	Twoâ€dimensional nearâ€infrared correlation spectroscopy studies of polymer blends I: Compositionâ€dependent spectral variations of blends of atactic polystyrene and poly[2,6â€dimethylâ€1,4â€phenylene ether]. Macromolecular Symposia, 1999, 141, 167-183.	0.4	6
384	Dynamic Enhanced Vibrational Spectroscopy of Molecules in Near Field The Review of Laser Engineering, 1999, 27, 703-707.	0.0	0
385	NIR SERS detection of immune reaction on gold colloid particles without bound/free antigen separation. Journal of Raman Spectroscopy, 1998, 29, 739-742.	1.2	43
386	Age and regional structural characterization of lipid hydrocarbon chains from human lenses by infrared, and near-infrared raman, spectroscopies. Biospectroscopy, 1998, 2, 113-123.	0.4	9
387	Determination of human serum albumin and Î ³ -globulin in a control serum solution by near-infrared spectroscopy and partial least squares regression. Fresenius' Journal of Analytical Chemistry, 1998, 362, 155-161.	1.5	22
388	Molecular Orientation and Aggregation in Mixed Langmuirâ^'Blodgett Films of 5-(4-N-Octadecylpyridyl)-10,15,20-tri-p-tolylporphyrin and Stearic Acid Studied by Ultravioletâ^'Visible, Fluorescence, and Infrared Spectroscopies. Langmuir, 1998, 14, 1177-1182.	1.6	35
389	IR and AFM Studies on Aging Effects of One-layer Langmuir-Blodgett Films of 2-Alkyl-7,7,8,8-tetracyanoquinodimethane. Molecular Crystals and Liquid Crystals, 1998, 322, 215-220.	0.3	2
390	Potential of twoâ€dimensional nearâ€infrared correlation spectroscopy in studies of preâ€melting behavior of nylon 12. Macromolecular Symposia, 1997, 119, 49-63.	0.4	9
391			

#	Article	IF	CITATIONS
397	Quantitative analysis of metabolites in urine by anti-Stokes Raman spectroscopy. Biospectroscopy, 1997, 3, 113-120.	0.4	16
398	FTIR studies of conformational energies of poly(acrylic acid) in cast films. , 1997, 35, 507.		1
399	The Nondestructive Identification of Ivory-Like Seal Materials. Journal of Forensic Sciences, 1997, 42, 434-436.	0.9	4
400	Highly Sensitive Gas Analysis by Raman Spectroscopy and its Application The Review of Laser Engineering, 1997, 25, 697-701.	0.0	0
401	Two-Dimensional Correlation Spectroscopy Study of Temperature-Dependent Spectral Variations ofN-Methylacetamide in the Pure Liquid State. 1. Two-Dimensional Infrared Analysis. The Journal of Physical Chemistry, 1996, 100, 8665-8673.	2.9	91
402	Two-Dimensional Correlation Spectroscopy Study of Temperature-Dependent Spectral Variations ofN-Methylacetamide in the Pure Liquid State. 2. Two-Dimensional Raman and Infraredâ^'Raman Heterospectral Analysis. The Journal of Physical Chemistry, 1996, 100, 8674-8680.	2.9	104
403	Thermal Behavior of Wixed-Stack Charge Transfer Films of 2-Octadecyl-7,7,8,8-tetracyanoquinodimethane and 3,3â€~,5,5â€~-Tetramethylbenzidine Prepared by the Langmuirâ^'Blodgett Technique and Donor Doping. 2. Morphology and Annealing Effects of the Films Investigated by Atomic Force Microscopy and Ultravioletâ^'Visibleâ^'Near Infrared and Infrared	2.9	24
404	Spectroscopies. The Journal of Physical Chemistry, 1996, 1997, 1998, 1998, 1998. Age and regional structural characterization of lipid hydrocarbon chains from human lenses by infrared, and nearâ€infrared raman, spectroscopies. Biospectroscopy, 1996, 2, 113-123.	0.4	17
405	FTâ€NIR Spectroscopy of some longâ€chain fatty acids and alcohols. Macromolecular Symposia, 1995, 94, 51-59.	0.4	14
406	Near Infrared Spectroscopy and Chemometrics Studies of Temperature-Dependent Spectral Variations of Water: Relationship between Spectral Changes and Hydrogen Bonds. Journal of Near Infrared Spectroscopy, 1995, 3, 191-201.	0.8	198
407	INTERCONVERSION OF BACTERIOCHLOROPHYLL c AGGREGATES IN SOLID FILMS UPON ORGANIC VAPOR TREATMENT. Photochemistry and Photobiology, 1995, 62, 496-501.	1.3	8
408	NEAR-INFRARED-FT-RAMAN STUDY OF AGGREGATION OF BACTERIOCHLOROPHYLL c IN WHOLE LIVING Chlorobium limicola. Photochemistry and Photobiology, 1995, 62, 509-513.	1.3	5
409	NEAR-INFRARED FOURIER-TRANSFORM RAMAN STUDY OF CHLOROPHYLL a IN SOLUTIONS. Photochemistry and Photobiology, 1995, 61, 175-182.	1.3	13
410	Self-Association of cis-9-Octadecen-1-ol in the Pure Liquid State and in Decane Solutions As Observed by Viscosity, Self-Diffusion, Nuclear Magnetic Resonance, Electron Spin Resonance, and Near-Infrared Spectroscopic Measurements. The Journal of Physical Chemistry, 1995, 99, 4155-4161.	2.9	33
411	Near-IR molar absorption coefficient for the OH-stretching mode of cis-9-octadecenoic acid and dissociation of the acid dimers in the pure liquid state. Journal of the Chemical Society, Faraday Transactions, 1995, 91, 697.	1.7	50
412	Structural characterization of clear human lens lipid membranes by near-infrared Fourier transform Raman spectroscopy. Current Eye Research, 1995, 14, 511-515.	0.7	16
413	Are the integrated absorption coefficients temperature dependent? FT-NIR study of the first overtone of the OH stretching mode of octanoic acid. Spectrochimica Acta Part A: Molecular Spectroscopy, 1994, 50, 1521-1528.	0.1	17
414	The formation and characterization of the in vitro polymeric aggregates of bacteriochlorophyllc homologs fromChlorobium limicola in aqueous suspension in the presence of monogalactosyl diglyceride. Photosynthesis Research, 1994, 41, 235-243.	1.6	68

#	Article	IF	CITATIONS
415	Near-infrared Fourier transform Raman spectroscopic study of human brain tissues and tumours. Journal of Raman Spectroscopy, 1994, 25, 25-29.	1.2	116
416	Studies on Spectra/Structure Correlations in Near-Infrared Spectra of Proteins and Polypeptides. Part I: A Marker Band for Hydrogen Bonds. Applied Spectroscopy, 1994, 48, 1249-1254.	1.2	73
417	Ceneration of the topa quinone cofactor in bacterial monoamine oxidase by cupric ion-dependent autooxidation of a specific tyrosyl residue. FEBS Letters, 1994, 351, 360-364.	1.3	175
418	Use of Principal Component Analysis in a near Infrared Study of the Dissociation Process of Oleyl Alcohol. Journal of Near Infrared Spectroscopy, 1994, 2, 137-143.	0.8	1
419	Quantitative Study of the Dissociation of Dimeric cis-9, cis-12-Octadecadienoic Acid in Pure Liquid by the FT-IR Liquid Film Technique. Applied Spectroscopy, 1993, 47, 2157-2161.	1.2	15
420	Potential of Fourier Transform Near-Infrared Spectroscopy in Studies of the Dissociation of Fatty Acids in the Liquid Phase. Applied Spectroscopy, 1993, 47, 2162-2168.	1.2	52
421	Temperature Dependent FT-IR and FT-Raman Studies of C60And C70in Solid States. Fullerenes, Nanotubes, and Carbon Nanostructures, 1993, 1, 329-338.	0.6	4
422	Raman structural characterization of clear human lens lipid membranes. Current Eye Research, 1993, 12, 279-284.	0.7	15
423	Dissociation of dimeric cis-9-octadecenoic acid in its pure liquid state as observed by near-infrared spectroscopic measurement. The Journal of Physical Chemistry, 1993, 97, 3129-3133.	2.9	53
424	Time-resolved FT-IR studyof 5-(2-fluoroalkoxy)-2-(4-n-alkylphenyl)-pyrimidine. Ferroelectrics, 1993, 147, 441-445.	0.3	11
425	Estimation of Structural Changes in the Cataractous Rat Lens Using Raman Spectroscopy. Experimental Animals, 1992, 41, 225-230.	0.7	1
426	Biological Applications of Near-infrared Excited Raman Spectroscopy The Review of Laser Engineering, 1992, 20, 889-898.	0.0	0
427	Can near Infrared Spectroscopy Monitor Changes in the Secondary Structure of Proteins?. NIR News, 1992, 3, 10-11.	1.6	5
428	Acetic, propionic, and oleic acid as the possible factors influencing the predominant residence of some species of <i>Propionibacterium</i> and coagulase-negative <i>Staphylococcus</i> on normal human skin. Canadian Journal of Microbiology, 1984, 30, 647-652.	0.8	58
429	Application to Agricultural Products and Foodstuff. , 0, , 269-287.		2
430	Near-Infrared FT-Raman Spectroscopy. , 0, , 85-114.		0
431	Sampling and Sample Presentation. , 0, , 115-124.		3
432	Applications to Polymers and Textiles. , 0, , 213-245.		2

Applications to Polymers and Textiles. , 0, , 213-245. 432

#	Article	IF	CITATIONS
433	Application to Industrial Process Control. , 0, , 247-268.		1
434	Applications of Near-Infrared Spectroscopy in Medical Sciences. , 0, , 289-333.		10
435	New Techniques in Near-Infrared Spectroscopy. , 0, , 75-84.		2
436	Instrumentation for Near-Infrared Spectroscopy. , 0, , 43-73.		2
437	Phase-Transitions in Langmuir-Blodgett and Cast Films of a Ferroelectric Liquid Crystal. , 0, , .		0